Chirality Transfer in 1D Self-Assemblies: Influence of H-Bonding vs Metal Coordination between Dicyano[7]helicene Enantiomers

Aneliia Shchyrba,[†] Manh-Thuong Nguyen,[‡] Christian Wäckerlin,[§] Susanne Martens,[†] Sylwia Nowakowska,[†] Toni Ivas,[†] Jesse Roose,[⊥] Thomas Nijs,[†] Serpil Boz,[†,¶] Michael Schär,[⊥] Meike Stöhr,[‖] Carlo A. Pignedoli,[#] Carlo Thilgen,[⊥] François Diederich,[⊥] Daniele Passerone,[#] and Thomas A. Jung*,[§]

[†]Department of Physics, University of Basel, Klingelbergstrasse 82, 4056 Basel, Switzerland

[‡]The Abdus Salam International Centre for Theoretical Physics, Strada Costiera 11, I-34151 Trieste, Italy

[§]Laboratory for Micro- and Nanotechnology, Paul Scherrer Institute, 5232 Villigen, Switzerland

[⊥]Laboratorium für Organische Chemie, ETH Zurich, Wolfgang-Pauli-Strasse 10, 8093 Zürich, Switzerland

[‖]Zernike Institute for Advanced Materials, University of Groningen, Nijenborgh 4, 9747 AG Groningen, The Netherlands

[#]Empa, Swiss Federal Laboratories for Materials Science and Technology, Überlandstrasse 129, CH-8600 Dübendorf, Switzerland

S *Supporting Information*

ABSTRACT: Chiral recognition as well as chirality transfer in supramolecular self-assembly and on-surface coordination is studied for the enantiopure 6,13-dicyano[7]helicene building block. It is remarkable that, with this helical molecule, both H-bonded chains and metal-coordinated chains can be formed on the same substrate, thereby allowing for a direct comparison of the chain bonding motifs and their effects on the self-assembly in experiment and theory. Conformational flexure and both adsorbate/adsorbent and intermolecular interactions can be identified as factors influencing the chiral recognition at the binding site. The observed H-bonded chains are chiral, however, the overall appearance of Cu-coordinated chains is no longer chiral. The study was performed via scanning tunneling microscopy, X-ray-photoelectron spectroscopy and density functional theory calculations. We show a significant influence of the molecular flexibility and the type of bonding motif on the chirality transfer in the 1D self-assembly.

Controlling and understanding chirality in chemical reactions and during self-assembly is important, in particular if chiral or pro-chiral building blocks are involved.[1,2] Recently, a Pasteur-type[3] spontaneous chiral resolution was shown to occur also in two dimensions, at surfaces.[2a,4] In analogy to the 3D case, the condensation of 2D islands at surfaces can be controlled by the enantiomeric excess[5] of one component or by a chiral auxiliary.[6] Chirality transfer and the long-range expression of chirality in molecular self-assembly have been studied intensively in surface science. These studies involved prochiral molecules[6,7] which become chiral upon conformational changes induced by their interaction with the substrate, as well as inherently chiral molecules. A very interesting model system is [n]helicenes, which have been used to study the chirality transfer during nucleation and self-assembly at the solid/liquid interface[8] as well as at the solid/vacuum interface.[9] No chiral interactions

were observed for layers of hexathia[11]helicene on Au(111) nor for linear ad molecular chains on Au(110).[10] Parschau et al. studied the chirality transfer of [7]helicene in the growth of 2D islands by van der Waals (vdW) interactions.[11] Later, Stöhr et al. showed the spontaneous resolution of (±)-6,13-dicyano[7]-helicene driven by polar interactions,[12] and Seibel et al. described the 2D separation of pentahelicene into homochiral domains purely through vdW forces.[13] Only a few investigations on chiral molecules self-assembling to structures of further reduced dimensionality, i.e. 1D, have been reported: On calcite, Kühnle et al. observed islands of enantiopure [7]helicene-2-carboxylic acid and chains of the racemate, both stabilized by $\pi-\pi$ stacking.[14] Here we report on the chirality transfer that takes place during the self-assembly of enantiopure dicyanohelicene building blocks into 1D chains, with particular focus on the influence of the intermolecular bonding motif.

With enantiomers of cyano-functionalized helicenes, (P)-(+)-6,13-dicyano[7]helicene and (M)-(−)-6,13-dicyano[7]-helicene ((P)-**1** and (M)-**1**, Figure 1), we earlier introduced an inherently chiral molecule with intermolecular bonding capability.[12] In this work we demonstrate that the intermolecular interactions can be tuned by the presence or absence of coordinating metal atoms, i.e. adatoms that can be supplied by
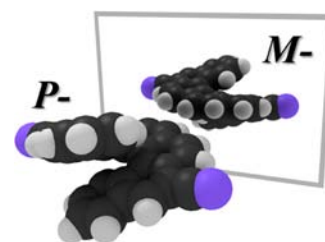
Figure 1. Enantiomers of 6,13-dicyano[7]helicene: (P)-**1** and its mirror image (M)-**1**.
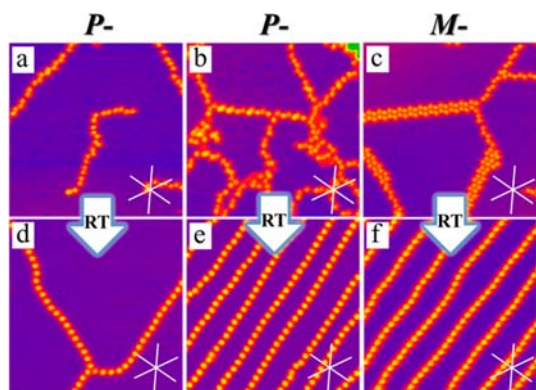
Figure 2. Top: Transition, upon heating, of self-assembled chains of enantiopure **1** created by deposition at low (a) and higher (b,c) coverages of (a,b) (P)-**1** or (c) (M)-**1** on cold (90 K) Cu(111) substrates. Here coverages are significantly smaller than in our previous work.[12] Bottom: Evolution of the chain morphology after heating to RT. STM images of enantiopure dicyano[7]helicenes taken at 5 K (30 × 30 nm², 25 pA, 1.2 V) reflect linear zigzag-shaped H-bonded self-assemblies and the subsequent formation of elongated islands at increased coverage created by deposition of (a,b) (P)-**1** and (c) (M)-**1** onto a Cu(111) substrate held at 90 K. (d−f) Formation of highly ordered molecular chains after annealing for 1 h at 300 K of the samples shown in (a−c). Chains of both chirality senses, (P)-**1** and (M)-**1**, are oriented 30° off the Cu(111) high-symmetry directions (indicated by white stars in each STM image).

Figure 3. (a) XPS of submonolayer coverage of (P)-**1** on Cu(111) (green) and Au(111) before (blue) and after (red) Cu addition. The presence of Cu adatoms significantly increases the N1s BE, confirming the formation of a Cu coordination complex. (b) STM image (35 × 35 nm², 77 K) revealing Cu-coordinated (P)-**1** chains on Au(111), oriented along the linear domains of the herringbone reconstruction.[20] (c) High-resolution STM image (4.0 × 1.8 nm², 77 K) of two neighboring chains on the hcp-domain of the reconstructed Au(111) surface (cf. Figure S6).

means of deposition or by thermally activated release from the substrate. An irreversible conversion of 1D H-bonded assemblies of enantiomerically pure **1** to a Cu-coordinated chain assembly occurs. Surprisingly, in the H-bonded case, the opposite enantiomer leads to chains of inverted symmetry, whereas this is not the case for the metal-coordinated chains.

All samples were prepared and characterized in ultrahigh vacuum. Molecules were deposited onto the substrates held at 90 or 300 K. Morphological assignment of the self-assembled structures was performed via scanning tunneling microscopy (STM) at 5 K, unless mentioned otherwise, and the chemical environment of N-atoms in the CN-groups was characterized by X-ray photoelectron spectroscopy (XPS) at room temperature (RT). Complementary density functional theory (DFT) calculations are used to model possible supramolecular arrangements (see Supporting Information (SI) for experimental and computational details).

STM experiments, performed after deposition of enantiopure (P)-**1** or (M)-**1** on Cu(111) held at 90 K, reveal assemblies that are modified after heating to RT. STM images of enantiopure **1**, deposited on Cu(111) at 90 K, show a zigzag chain organization for (P)-**1** (Figure 2a,b) and (M)-**1** (Figure 2c). With increasing coverage, the well-separated zigzag chains (Figure 2a, ∼0.05 mol/nm²) evolve into irregular networks of chains and linear supramolecular islands (Figure 2b,c; ∼0.17 and ∼0.15 mol/nm², respectively). Interestingly, we observe the directions of the chains to be independent of the chirality sense of the constituent molecules, namely along the directions rotated by 30° with respect to the principal axis of the Cu(111) surface. Heating the samples to RT and re-investigating by STM at 5 K reveals a strongly modified morphology: only long and straight chains occur, oriented along the same crystallographic directions as before. The chain direction again does not change with chirality sense ((P)-**1**, Figure 2d,e/(M)-**1**, Figure 2f). The evolution of zigzag chains to linear chains has also been observed for the

racemic mixture (±)-**1** (cf. Figure S1). Importantly, at increased coverage, a new phase consists of large domains of parallel and quasi equidistant linear chains (cf. Figure S2). We attribute this to repulsive electrostatic interactions (Figure 2e,f; see also SI sections 4 and 10), as similarly assigned for Cu-pyridyl coordinated chains.[15] These complex phenomenological changes and the transition from chiral H-bonded zigzag chains to straight linear chains with overall lack of chiral appearance (*vide infra*) hint at modified chain binding motifs after annealing, in agreement with CN-Cu-assisted on-surface assembly.[16]

The chain architecture critically depends on intermolecular interactions. The zigzag structure of the chains formed at low (90 K) sample temperature can be tentatively attributed to a balance between H-bonding (C−H···NC) and vdW interactions. We performed an XPS study to investigate the nature of the interactions in the straight chain assembly. For this purpose, we sublimed (P)-**1** onto Cu(111) and Au(111) surfaces kept at 300 K. The N1s binding energies of (P)-**1** correspond to 398.85 eV for submonolayer coverage on Au(111) and 399.15 eV for a multilayer on Cu(111) (cf. Figures 3 and S4). These values correspond well with N1s XPS data for cyano substituents.[17] The significantly higher N1s binding energy (BE) for submonolayer coverage of (P)-**1** on Cu(111) (399.85 eV) evidences a different chemical environment of the nitrogen. Further, only one N1s peak is observed, revealing equal bonding of both CN groups. Notably, the lone-pair of the N atom might interact with the Cu substrate. However, sp-hybridization of the cyano nitrogen and energetically favorable σ-donor complexation to a metal (M) require a CN−M angle close to 180°. Thus, this arrangement with both cyano groups simultaneously pointing to the surface is barely feasible (cf. Figure 1). In the case of chemisorption of the CN groups and absence of their coordination, a N1s peak at lower BE would be expected.[18] Our observation of the N1s at higher BE provides experimental evidence for the involvement of Cu adatoms in intermolecular bonding and chain formation, supported by the STM manipulations and DFT calculations (cf. Figure S7 and SI section 12).

To confirm the presence of Cu adatoms in the straight chain architecture, we evaporated a trace amount (∼0.07 ML) of Cu onto the submonolayer of (P)-**1** on Au(111). In subsequently acquired XPS data, the N1s BE is shifted from 398.85 to 399.65 eV (Figure 3a). STM measurements performed on the same sample at 77 K show straight chains (Figure 3b).

Conversely, in the absence of trace amounts of Cu, STM at 77 K reveals only a 2D condensed phase (cf. Figure S5). These XPS and STM data confirm spontaneous coordination of (P)-**1** to Cu adatoms on Au(111). Notably, the Cu-coordinated chains are aligned along the herringbone reconstruction of the substrate (Figure 3b). In particular, the pair of chains in closer proximity (∼2 nm) can be located at the linear hcp-domains, and the single chain follows the fcc-domains of the reconstruction (cf. Figures 3c and S6). Another interesting feature is the considerable variation in the intermolecular distance when the chains reorient by following the domains of the surface reconstruction. The range of variation (∼1.2−1.5 nm ± 0.1 nm) is atypical for coordination complexes and may be attributed to the flexibility of the helicene backbone.

The observation of straight or zigzag chains dependent on the Cu(111) substrate temperature during deposition of (P)-**1** or (M)-**1** is consistent with the above-described observations of the Cu coordination occurring after deposition of Cu adatoms on Au(111) held at RT. Notably, we observed the coexistence of linear and zigzag chains after deposition of (P)-**1** on Cu(111) held at intermediate sample temperatures (∼130 K). The availability of Cu adatoms from surface self-diffusion on Cu(111) depends primarily on the temperature, among other factors. At the substrate temperature used to generate zigzag chains (90 K), the presence of Cu adatoms is significantly lowered;[19] at further elevated temperatures CN-Cu complexes modify the chain (SI section 5).

An important question with regard to the chirality of the building block relates to the degree of chirality transfer observable in the two different architectures, namely the H-bonded vs the Cu-coordinated chains of (P)-**1** or (M)-**1**. The H-bonded chains of homochiral molecules appear as imperfect regular arrangement of dimers. However, far less defects occur in the chain after coordination to Cu. This is attributed to the thermodynamics of the system after being annealed, as well as to higher BE of the coordination bonds in comparison to H-bonds. Moreover, H-bonding can involve different aryl H atoms resulting in an aperiodic chain.[21] The most important difference between the two chain architectures lies in the presence or absence of mirror symmetry. For the H-bonded chains, the chirality of enantiopure (P)-**1** or (M)-**1** is reflected in the H-bonding pattern as mirroring of the dimers making the chain (Figure 4a,c). In contrast, no such signature is observable after Cu coordination where the apparent repetitive unit consists of a single molecule only (Figure 4b,d).

DFT calculations were performed to complement the experimental observations on (M)-**1** for the H-bonded (Figure 4e) and Cu-coordinated chains (Figure 4f). The superimposed simulated and experimental STM data show good agreement. The calculations confirm the modification of the chain architecture (Figure 4e,f, cf. Figures S7−S9) with the transition of the bonding motif. As demonstrated in the side views in Figure 4e,f, the dimers of the H-bonded chain derive from close contact interactions (H-bond, preferred to CN−Cu bonding and vdW) between two helicene molecules, leading to two nonequivalent positions of the CN groups involved in the bonding. This nonequivalence implies that the chain exhibits a directional sense, and re-orientation of different segments within one chain is improbable due to the different angle formed by the CN groups with respect to the substrate, as observed in Figure 4e. After Cu coordination, this nonequivalence is lifted by the flexure of the molecule to bind to the equidistant Cu adatoms. It seems that the strong coordination bond forces the helicene into the inter-
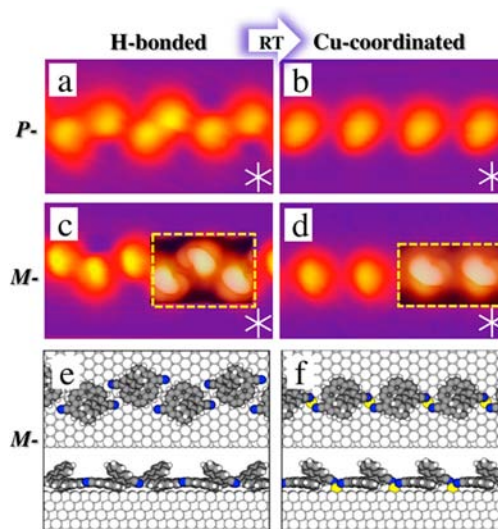
Figure 4. STM images (5.4 nm × 3.2 nm) of (a) (P)-**1** and (c) (M)-**1** on Cu(111) reveal a mirror-image appearance in H-bonded chains. After coordination with Cu adatoms, the chains have a similar appearance (b,d). Transition from one bonding motif to the other occurs upon annealing for 1 h at 300 K. Simulated STM images (marked by yellow dashed rectangles) of (c) H-bonded and (d) Cu-coordinated chains are superimposed onto the experimental ones. (e,f) DFT models for H-bonded and metal-coordinated (M)-**1** chains.

adatom gap which is determined by the lattice registry. This occurs for both enantiomers and also for the racemate (cf. Figure S1). The intermolecular distances, determined from STM data, increase from 1.00 nm for the H-bonded chains to 1.35 nm for the Cu-coordinated chains. Experimental results and calculations of the proposed models are in good qualitative and quantitative agreement (SI section 9).

Concerning the chirality transfer in supramolecular on-surface arrays, the two types of helicene chains provide a very interesting model system: the same molecule forms two different chain arrangements by either weak H-bonding or relatively stronger coordination bonds. In this context, it is important to discuss the intermolecular and molecule/substrate interactions with respect to the orientation of the building blocks within the chain. Note that all adsorbed helicenes of the same chirality sense can be aligned in the same manner by mere rotation and translation. Upon binding in a 1D chain, the CN groups are fixed to the nearest-neighbor molecules and exhibit a CN "tail" and a CN "head" with different angles with respect to the substrate. Thus, different arrangements within one chain are possible. Due to the geometric constraints of the H-bonded architecture, tail-to-tail and head-to-head connections are more plausible than tail-to-head connections. This preference is confirmed in the simulated minimal energy arrangement (Figure 4e, cf. Figure S9). Further evidence is provided by the regularity of chains formed from enantiopure helicenes in comparison to the irregular arrangement of the racemic H-bonded chain on the same substrate.

Switching the point symmetry (chirality sense) of the building block from (P)-**1** to (M)-**1** leads to exact mirroring of the self-assembled H-bonded chains: the characteristic "dimers" recognized in the STM data are symmetry-inverted. The overall "chain direction" with respect to the surface, however, remains the same. We attribute this observation to the high symmetry of the chain directions, i.e. $\langle 11\bar{2} \rangle$ family of directions, which are mapped onto themselves upon symmetry inversion. After Cu coordination of the enantiopure (P)-**1** or (M)-**1**, the character-

istic image of the chain is modified, and two different orientations of the building blocks in the chain arrangement can be observed. These orientations are observed in random distribution, so all possible combinations occur: head−head, head−tail, and tail−tail (Figure S12). This behavior indicates that the coordination bond, unlike the H-bond, does not differentiate head−tail, head−head, and tail−tail connections; thus, we do not observe mirror-image patterns in enantiopure Cu-coordinated chains. The racemic helicene forms Cu-coordinated chains along the same $\langle 11\bar{2}\rangle$ directions. Stereoselectivity, a key factor in the assembly of the H-bonded chain, becomes negligible due to the strong influence of the metal coordination bond. This is confirmed in the numerical calculations by the limited flexure in H-bonded chains leading to nonequivalent bonding and by the considerable flexure of the helicenes after the stronger coordination bond is formed. This stronger binding in the chain (i) flexes helicenes, (ii) directs the chain formation despite small energy differences stemming from the different binding motifs (i.e., 3^2 for a racemate), and (iii) overcomes nonequivalences in the molecular footprint of helicene on the corrugated substrate between the adatoms.

In general, molecular superstructures comprised of chiral elements on any surface give rise to mirror-inverted structures when the element of opposite chirality sense is used.[2] Our work demonstrates a remarkable exception, as the direction of helicene chains is independent of the chirality sense (*P* or *M*) of the molecular building block—neither in the case of the H-bonded nor the Cu-coordinated chain. However, locally we observe that the symmetry of the H-bonded dimers is mirrored when the helicene of opposite chirality sense is used. By Cu coordination, the tolerance to symmetry and registry defects is observed to increase considerably. Thus, no spontaneous resolution is expected for 1D arrangements formed by Cu coordination. In conclusion, the complexity of intermolecular interactions—in the present case flexibility and weaker H-bonding vs stronger Cu coordination—significantly affects the possibility of chiral recognition and spontaneous resolution.

■ ASSOCIATED CONTENT

Ⓢ Supporting Information
STM, XPS, and DFT methods and analyses. This material is available free of charge via the Internet at http://pubs.acs.org.

■ AUTHOR INFORMATION

Corresponding Author
thomas.jung@psi.ch

Present Address
¶Faculty of Engineering, Gedik University, 34876, Kartal, Istanbul, Turkey.

Notes
The authors declare no competing financial interest.

■ ACKNOWLEDGMENTS

contribution to the graphics. The STM data were processed with the WSXM software.[22]

■ REFERENCES

(1) Shen, Y.; Chen, C.-F. *Chem. Rev.* **2012**, *112*, 1463.
(2) (a) Ernst, K.-H. *Phys. Status Solidi B* **2012**, *249*, 2057. (b) Gingras, M. *Chem. Soc. Rev.* **2013**, *42*, 1051.
(3) Flack, H. D. *Acta Crystallogr. A* **2009**, *65*, 371.
(4) (a) Santagata, N. M.; Lakhani, A. M.; Davis, B. F.; Luo, P.; Buongiorno Nardelli, M.; Pearl, T. P. *J. Phys. Chem. C* **2010**, *114*, 8917. (b) Ortega Lorenzo, M.; Baddeley, C. J.; Muryn, C.; Raval, R. *Nature* **2000**, *404*, 376. (c) Barlow, S. M.; Louafi, S.; Le Roux, D.; Williams, J.; Muryn, C.; Haq, S.; Raval, R. *Langmuir* **2004**, *20*, 7171.
(5) (a) Parschau, M.; Romer, S.; Ernst, K.-H. *J. Am. Chem. Soc.* **2004**, *126*, 15398. (b) Parschau, M.; Kampen, T.; Ernst, K.-H. *Chem. Phys. Lett.* **2005**, *407*, 433.
(6) De Cat, I.; Guo, Z.; George, S. J.; Meijer, E. W.; Schenning, A. P. H. J.; De Feyter, S. *J. Am. Chem. Soc.* **2012**, *134*, 3171.
(7) Mugarza, A.; Lorente, N.; Ordejón, P.; Krull, C.; Stepanow, S.; Bocquet, M.-L.; Fraxedas, J.; Ceballos, G.; Gambardella, P. *Phys. Rev. Lett.* **2010**, *105*, 115702.
(8) Balandina, T.; van der Meijden, M. W.; Ivasenko, O.; Cornil, D.; Cornil, J.; Lazzaroni, R.; Kellogg, R. M.; De Feyter, S. *Chem. Commun.* **2013**, *49*, 2207.
(9) (a) Fasel, R.; Parschau, M.; Ernst, K.-H. *Angew. Chem. Int. Ed.* **2003**, *42*, 5178. (b) Fasel, R.; Parschau, M.; Ernst, K.-H. *Nature* **2006**, *439*, 449.
(10) Taniguchi, M.; Nakagawa, H.; Yamagishi, A.; Yamada, K. *J. Mol. Catal. A Chem.* **2003**, *199*, 65.
(11) Parschau, M.; Fasel, R.; Ernst, K.-H. *Cryst. Growth Des.* **2008**, *8*, 1890.
(12) Stöhr, M.; Boz, S.; Schär, M.; Nguyen, M.-T.; Pignedoli, C. A.; Passerone, D.; Schweizer, W. B.; Thilgen, C.; Jung, T. A.; Diederich, F. *Angew. Chem. Int. Ed.* **2011**, *50*, 9982.
(13) Seibel, J.; Allemann, O.; Siegel, J. S.; Ernst, K.-H. *J. Am. Chem. Soc.* **2013**, *135*, 7434.
(14) (a) Hauke, C. M.; Rahe, P.; Nimmrich, M.; Schütte, J.; Kittelmann, M.; Stará, I. G.; Starý, I.; Rybáček, J.; Kühnle, A. *J. Phys. Chem. C* **2012**, *116*, 4637. (b) Rahe, P.; Nimmrich, M.; Greuling, A.; Schütte, J.; Stará, I. G.; Rybáček, J.; Huerta-Angeles, G.; Starý, I.; Rohlfing, M.; Kühnle, A. *J. Phys. Chem. C* **2010**, *114*, 1547. (c) Rybáček, J.; Huerta-Angeles, G.; Kollárovič, A.; Stará, I. G.; Starý, I.; Rahe, P.; Nimmrich, M.; Kühnle, A. *Eur. J. Org. Chem.* **2011**, *2011*, 853.
(15) Heim, D.; Écija, D.; Seufert, K.; Auwärter, W.; Aurisicchio, C.; Fabbro, C.; Bonifazi, D.; Barth, J. V. *J. Am. Chem. Soc.* **2010**, *132*, 6783.
(16) (a) Pawin, G.; Wong, K. L.; Kim, D.; Sun, D.; Bartels, L.; Hong, S.; Rahman, T. S.; Carp, R.; Marsella, M. *Angew. Chem. Int. Ed.* **2008**, *47*, 8442. (b) Sirtl, T.; Schlögl, S.; Rastgoo-Lahrood, A.; Jelic, J.; Neogi, S.; Schmittel, M.; Heckl, W. M.; Reuter, K.; Lackinger, M. *J. Am. Chem. Soc.* **2013**, *135*, 691. (c) Pivetta, M.; Pacchioni, G. E.; Schlickum, U.; Barth, J. V.; Brune, H. *Phys. Rev. Lett.* **2013**, *110*, 086102.
(17) Lindberg, B. J.; Hedman, J. *Chem. Scr.* **1975**, *7*, 155.
(18) (a) Sexton, B. A.; Hughes, A. E. *Surf. Sci.* **1984**, *140*, 227. (b) Piantek, M.; Miguel, J.; Krüger, A.; Navío, C.; Bernien, M.; Ball, D. K.; Hermann, K.; Kuch, W. *J. Phys. Chem. C* **2009**, *113*, 20307.
(19) Wang, W.; Shi, X.; Wang, S.; Van Hove, M. A.; Lin, N. *J. Am. Chem. Soc.* **2011**, *133*, 13264.
(20) (a) Fernandez-Torrente, I.; Monturet, S.; Franke, K.; Fraxedas, J.; Lorente, N.; Pascual, J. *Phys. Rev. Lett.* **2007**, *99*, 176103. (b) Böhringer, M.; Morgenstern, K.; Schneider, W.-D.; Wühn, M.; Wöll, C.; Berndt, R. *Surf. Sci.* **2000**, *444*, 199. (c) Yu, M.; Kalashnyk, N.; Barattin, R.; Benjalal, Y.; Hliwa, M.; Bouju, X.; Gourdon, A.; Joachim, C.; Lægsgaard, E.; Besenbacher, F.; Linderoth, T. R. *Chem. Commun.* **2010**, *46*, 5545.
(21) Wintjes, N.; Hornung, J.; Lobo-Checa, J.; Voigt, T.; Samuely, T.; Thilgen, C.; Stöhr, M.; Diederich, F.; Jung, T. A. *Chem.—Eur. J.* **2008**, *14*, 5794.
(22) Horcas, I.; Fernández, R.; Gómez-Rodríguez, J. M.; Colchero, J.; Gómez-Herrero, J.; Baro, A. M. *Rev. Sci. Instrum.* **2007**, *78*, 013705.